

**ELECTROMAGNETIC WAVE PROPAGATION THROUGH A  
PLASMA SLAB: ANALYSIS OF REFLECTION,  
TRANSMISSION AND ABSORPTION CHARACTERISTICS FOR  
VARYING MEDIUMS**

A DISSERTATION  
SUBMITTED IN PARTIAL FULFILMENT OF THE REQUIREMENTS  
FOR THE AWARD OF THE DEGREE  
OF

**MASTER OF SCIENCE  
IN  
PHYSICS**

Submitted By:  
**Aditi Sharma**  
(2K23/MSCPHY/03)  
&  
**Diya**  
(2K23/MSCPHY/21)

Under the supervision of  
**Prof. Suresh C. Sharma**  
(Delhi Technological University)



**Department of Applied Physics**  
**DELHI TECHNOLOGICAL UNIVERSITY**

(Formerly Delhi College of Engineering)

Shahbad Daultpur, Main Bawana Road, Delhi-110042, India

**May, 2025**



**DELHI TECHNOLOGICAL UNIVERSITY**  
(Formerly Delhi College of Engineering)  
Bawana Road, Delhi-110042

## **CANDIDATE'S DECLARATION**

We, **Aditi Sharma (2K23/MSCPHY/03)** and **Diya (2K23/MSCPHY/21)** hereby certify that the work which is presented in the Dissertation-II entitled in fulfillment of the requirement for the award of the Master in Science in **Physics** and submitted to the Department of Applied Physics, Delhi Technological University, Delhi is an authentic record of our own, carried out during a period from August 2024 to May 2025 under the supervision of **Prof. Suresh C. Sharma**. The matter presented in this report/thesis has not been submitted by us for the award of any other degree of this or any other Institute/University.

**Title of the Paper:** Electromagnetic Wave Propagation Through A Plasma Slab: Analysis Of Reflection, Transmission, And Absorption Characteristics For Varying Mediums

**Author Names (in sequence as per research paper):** Diya, Aditi Sharma, Suresh C. Sharma

**Name of the Journal:** Journal Of Optics (Scopus Indexed)

**Status of paper:** Under Review

**Place:** Delhi

**Date:** 09/06/2025

A handwritten signature in blue ink, appearing to read 'Sharma', with a horizontal line extending from the end.

**Aditi Sharma**  
(2K23/MSCPHY/03)

A handwritten signature in blue ink, appearing to read 'Diya', with a horizontal line extending from the end.

**Diya**  
(2K23/MSCPHY/21)



**DELHI TECHNOLOGICAL UNIVERSITY**  
(Formerly Delhi College of Engineering)  
Bawana Road, Delhi-110042

**SUPERVISOR CERTIFICATE**

I hereby certify that the Project Dissertation titled “Electromagnetic Wave Propagation Through A Plasma Slab: Analysis Of Reflection, Transmission, And Absorption Characteristics For Varying Mediums” which is submitted by Aditi Sharma (2k23/MSCPHY/03) and Diya (2k23/MSCPHY/21), Delhi Technological University, Delhi in partial fulfillment of the requirement for the award of the degree of Master of Science Physics, is a record of the project work carried out by the students under my supervision. To the best of my knowledge this work has not been submitted in part or full for any Degree or Diploma to this University or elsewhere.

**Place:** Delhi

**Date:** 09/06/2025

A handwritten signature in blue ink, which appears to read "Suresh C. Sharma".

**Prof. Suresh C. Sharma**

**(SUPERVISOR)**



**DELHI TECHNOLOGICAL UNIVERSITY**  
(Formerly Delhi College of Engineering)  
Bawana Road, Delhi-110042

**ABSTRACT**

This paper presents a theoretical investigation of the reflection (R), transmission (T), and absorption (A) coefficients of electromagnetic waves interacting with a slab of plasma, complex dielectric and hydrogel. Starting with the calculation of the net phase acquired by the wave upon entering the slab, we derive the wave vector components and the dispersion relation governing the system. Using these, analytical expressions for R, T, and A are obtained by applying Maxwell's boundary conditions at the interfaces. Numerical simulations are carried out for various materials, including hydrogels and conventional dielectric media, to study and compare their electromagnetic responses. The results reveal distinct differences in wave behaviour due to varying medium-induced modifications in plasma permittivity. Theoretical predictions are validated by comparison with existing experimental data, demonstrating good agreement and highlighting the significant role of diverse mediums in controlling wave propagation. This work provides insights into the design of plasma-based devices for electromagnetic filtering and shielding applications.



**DELHI TECHNOLOGICAL UNIVERSITY**  
(Formerly Delhi College of Engineering)  
Bawana Road, Delhi-110042

## **ACKNOWLEDGEMENT**

First and foremost, we would like to express our heartfelt and sincere gratitude to our supervisor, **Prof. Suresh C. Sharma**, Department of Applied Physics, Delhi Technological University for their inspiring guidance, constructive criticism, and valuable suggestions throughout the project. Without his mentoring and unconditional support, this work would not have been possible. We would also like to thank Mr Himank Sagar, Research Fellow, Plasma and Nano Simulation Lab, Department of Applied Physics, Delhi Technological University for his mentorship and for sharing his experience and expertise on this subject. We are thankful for his constant guidance and support. We are profoundly indebted to our parents and families, whose unconditional love, support, and encouragement have been our constant source of strength through all circumstances in life. Lastly, we are deeply grateful to God for His blessings, which have manifested through the support of all these wonderful individuals who have played a crucial role in helping us achieve this milestone.

A handwritten signature in blue ink that reads "Sharma".

**Aditi Sharma**  
(2K23/MSCPHY/03)

A handwritten signature in blue ink that reads "Diya".

**Diya**  
(2K23/MSCPHY/21)

# CONTENTS

<b>Candidate's Declaration</b>	<b>ii</b>
<b>Supervisor Certificate</b>	<b>iii</b>
<b>Abstract</b>	<b>iv</b>
<b>Acknowledgement</b>	<b>v</b>
<b>Contents</b>	<b>vi</b>
<b>List of figures</b>	<b>viii</b>

## **CHAPTER 1 INTRODUCTION.....1-6**

<b>1.1 Background and Motivation</b>	
<b>1.2 Applications of EM Wave interaction with Plasma and Complex media</b>	
<b>1.3 Literature Review</b>	
<b>1.4 Theoretical Background</b>	
<b>1.4.1 Plasma and Two-Stream Model</b>	
<b>1.4.2 Complex Dielectric Media</b>	
<b>1.4.3 Hydrogels as Electromagnetic Media</b>	
<b>1.4.4 Electromagnetic Waves: TE and TM Modes</b>	
<b>1.4.5 Maxwell's Boundary Conditions and Wave Coefficients</b>	
<b>1.5 Scope and Objectives of the Present Work</b>	

## **CHAPTER 2 ANALYTICAL MODELING AND COMPUTATIONAL APPROACH.....7-13**

<b>2.1 Mathematical Analysis</b>	
<b>2.2 Numerical Implementation</b>	
<b>2.2.1 Simulation Goals</b>	

### 2.2.2 *Simulation Environment (MATLAB)*

### 2.2.3 *Input Parameters*

### 2.2.4 *Outputs*

## **CHAPTER 3 RESULTS AND DISCUSSION.....14-25**

### **3.1 Reflection and Transmission Coefficients for Gaussian Wave on Plasma Interface**

### **3.2 Reflection and Transmission Coefficients as a function of relative permittivity**

### **3.3 Variation of Dielectric Constant of Hydrogel with Phase Shift**

### **3.4 Reflection, Transmission, and Absorption Coefficients for p-Polarized Waves in Plasma**

### **3.5 Reflection transmission coefficient as functions of the imaginary part of the dielectric constant**

### **3.6 Reflection and Transmission Coefficients vs Real Part of Dielectric Constant**

### **3.7 Reflection, Transmission, and Absorption Coefficients of Complex Dielectric**

## **CHAPTER 4 CONCLUSION.....26-28**

### **4.1 Summary of Findings**

### **4.2 Implications and Future Scope**

## **CHAPTER 5 REFERENCES.....29**

## **CHAPTER 6 PLAGIARISM REPORT.....31**

## **APPENDICES.....33**

## **LIST OF FIGURES**

<b>Figure 1</b>	MATLAB Interface	<b>12</b>
<b>Figure 2</b>	MATLAB Logo	<b>12</b>
<b>Figure 3</b>	Reflection and Transmission Coefficients as a function of incident Gaussian wave	<b>15</b>
<b>Figure 4</b>	Reflection and Transmission Coefficients as a function of relative permittivity	<b>17</b>
<b>Figure 5</b>	Variation of Dielectric Constant of Hydrogels with Phase Shift	<b>18</b>
<b>Figure 6</b>	Reflection, Transmission and Absorption Coefficients as a function of incident p-polarized wave for plasma	<b>20</b>
<b>Figure 7</b>	Reflection and Transmission Coefficients as function of imaginary part of dielectric constant	<b>22</b>
<b>Figure 8</b>	Reflection and Transmission Coefficients as a function of real dielectric constant	<b>23</b>
<b>Figure 9</b>	Reflection, Transmission, and Absorption Coefficients vs Imaginary Part of Dielectric Constant	<b>25</b>



# CHAPTER 1

## INTRODUCTION

### 1.1 Background and Motivation

The behavior of electromagnetic (EM) waves in plasma media has become a key topic in contemporary electrodynamics because of its extensive applications in space communication, nuclear fusion, remote sensing, and photonic devices. Of especial significance is the analysis of reflection (R), transmission (T), and absorption (A) of EM waves, particularly laser radiation, when it interacts with inhomogeneous or dispersive media like plasmas, dielectrics, or hydrogels. Plasmas, being ionized gases with free-moving ions and electrons, possess distinct dispersive characteristics that enable them to interact with electromagnetic waves in complicated manners. The interaction is even more complex when the plasma is composed of different species with varying drift velocities, a situation referred to as two-stream plasma. This configuration brings about anisotropy and streaming instabilities, influencing the optical characteristics and allowing for wave phenomena of total reflection, resonance transmission, and absorption-selective filtering. In this research work, the theoretical modeling of EM wave interaction with a plasma slab confined between  $z=0$  and  $z=d$  is considered. The system consists of electrons and ions with different velocities, inducing two-stream effects. The study is also taken up in complex dielectrics and hydrogels, which are materials of interest because they have a frequency-dependent dielectric response and can be explored for tunable EM applications. These materials together offer a diverse platform for studying medium-induced changes in wave propagation.

### 1.2 Applications of EM Wave interaction with Plasma and Complex media

The coupling of electromagnetic (EM) waves and plasma and multidomain media has many real-world applications, especially through the examination of reflection (R), transmission (T), and absorption (A) coefficients. In plasma diagnostics, reflection or transmission variations are used to deduce important plasma parameters like density,

temperature, and flow velocity [1, 2]. This is paramount for evaluating plasma behavior in laboratory as well as astrophysical environments. Within the area of laser-plasma interactions, more specifically within the context of Inertial Confinement Fusion (ICF), the understanding of energy coupling into plasma layers is key to realizing efficient implosion dynamics [3,4]. Photonic devices like plasma-based filters, mirrors, and metamaterials also utilize hydrogel and complex dielectric tunable optical properties to realize performance and function enhancement [5]. Stealth technology and plasma antenna systems are also enabled by this work, since control of reflection and absorption via velocity and permittivity adjustments allows for innovative solutions in adaptive electromagnetic shielding [6–10]. Hydrogels, with their high water content and tunable dielectric constants, also offer promising opportunities for developing bio-inspired EM absorbers and filters. When incorporated into stratified or multilayered structures, these materials have the potential to enhance or complement plasma-layered structures, expanding the possibilities of electromagnetic response engineering.

### 1.3 Literature Review

The early work by Hosono and Yamaguchi applied multistream plasma models to examine the effect of two or more charged species on reflection behavior and found differences in particle velocities can have a considerable effect on reflection and transmission profiles [11]. Building upon this foundation, this work takes a two-stream model—a simplified but useful framework—for examining such nonlinear interactions. Subsequent studies have expanded on these findings. Singh and Varma studied traveling, hot, magnetized plasmas and proved both drift velocity and temperature strongly modulate reflectivity [12]. Similarly, Walker examined MHD wave interactions between counter-streaming plasmas and discovered conditions conducive to generating negative energy waves [13]. Hojo et al. made a groundbreaking theory on Fabry–Perot resonance in plasma slabs, showing the possibility of reflectionless transmission under specific structural and frequency conditions [14]. Later, Rahmani et al. extended the above findings to inhomogeneous, magnetized plasmas and proved how electromagnetic responses can be engineered using external magnetic fields and collisional profiles [15]. Computational methods

such as the SO-FDTD technique have also enabled simulations of wave propagation in cold plasmas with spatially inhomogeneous densities [16].

To address the complex dynamics, foundational texts such as Born and Wolf's *Principles of Optics* [17] and Jackson's *Classical Electrodynamics* [18] have been instrumental in building the theoretical underpinnings. Works like Yeh (1988) on multilayered media [19], Rukhadze and Silin (1964) on electromagnetic properties of plasmas [20], and Milonni and Eberly (2010) on laser physics [21] further solidify the physical context. Other relevant contributions include studies on scattering in stratified plasmas, electromagnetic response of core-shell clusters [22], and analytical modeling of EM properties in complex media [23-26]. Furthermore, wave propagation in dielectric slabs and hydrogel has been investigated in order to examine permittivity-dependent control processes— an area also addressed in this work [27].

## 1.4 Theoretical Background

### 1.4.1 Plasma and Two-Stream Model

Plasma is also known as the fourth state of matter, and it is a quasi-neutral mixture of free electrons and ions. Plasma has collective behavior because of long-range electromagnetic interactions, and it is highly responsive to electric and magnetic fields. The basic property that describes a plasma is the plasma frequency ( $\omega_p$ ), which is the natural frequency at which electrons in a plasma oscillate in response to a perturbation. The permittivity of plasma is typically complex and frequency-dependent, and for a cold, collisionless, and unmagnetized plasma, it can be expressed as:

$$\varepsilon(\omega) = 1 - \frac{\omega_p^2}{\omega^2} \quad (1.1)$$

In more complicated situations, such as two-stream plasmas, there are two groups of charged particles (commonly electrons and ions) drifting at varying speeds. This creates anisotropy and generates streaming instabilities, influencing the wave propagation of electromagnetic waves. Such two-stream effects alter the dielectric response of the medium and change reflection and transmission properties [11].

### 1.4.2 Complex Dielectric Media

A dielectric medium is a material that can be polarized by an electric field but does not conduct electricity at standard circumstances. Dielectrics are normally linear or nonlinear, lossy or lossless, depending on the material composition and their reaction to electromagnetic waves.

A complex dielectric is one where the permittivity  $\varepsilon = \varepsilon' + i\varepsilon''$  has both real ( $\varepsilon'$ ) and imaginary ( $\varepsilon''$ ) parts. The real part determines the phase velocity of the wave and the imaginary part represents absorption or loss within the material.

Such complex media play a key role in understanding electromagnetic wave's attenuation and scattering in actual systems and are usually simulated to model engineered materials such as lossy polymers, semiconductors, or biological tissues.

### 1.4.3 Hydrogels as Electromagnetic Media

Hydrogels are elastic, water-absorbing polymeric materials that possess high dielectric tunability, biocompatibility, and mechanical elasticity. Hydrogels are tunable in their dielectric properties with regards to water content, temperature, and composition and are hence very promising devices for electromagnetic wave control.

Here, hydrogels are taken along with plasmas and conventional dielectrics to understand how different material responses influence reflection (R), transmission (T), and absorption (A) coefficients. Hydrogels can be used in bio-integrated sensors, wave absorbers, or reconfigurable photonic devices.

### 1.4.4 Electromagnetic Waves: TE and TM Modes

When electromagnetic waves propagate through a medium and encounter a boundary, their interaction is strongly affected by their polarization. The two most fundamental modes of polarization are:

- TE (Transverse Electric) Mode: The electric field is entirely transverse to the direction of propagation i.e.  $E_z=0$ , and the electric field lies in the plane perpendicular to the direction of wave travel.
- TM (Transverse Magnetic) Mode: The magnetic field is entirely transverse i.e.  $H_z=0$ , and the electric field has a component along the propagation direction.

These modes determine how the electromagnetic wave interacts with layered structures or inhomogeneous media. The reflection and transmission coefficients will vary depending on whether the incident wave is TE or TM polarized.

#### 1.4.5 Maxwell's Boundary Conditions and Wave Coefficients

The foundation of the analysis of any electromagnetic wave interaction is Maxwell's equations. Maxwell's equations-derived boundary conditions are used in the two-media interfaces to equate electric and magnetic field tangential components. Continuity equations are used to derive reflection coefficient (R) and transmission coefficient (T).

In general:

- The reflection coefficient R is defined as the ratio of the amplitude of the reflected field to the incident field.
- The transmission coefficient T is the ratio of the transmitted field amplitude to the incident field amplitude.
- The absorption coefficient A is determined from energy conservation:

$$A = 1 - |R|^2 - |T|^2 \quad (1.2)$$

These coefficients will depend on the angle of incidence, wave frequency, and the electromagnetic properties (permittivity and permeability) of the media. Analytical forms for R, T, and A are required to explain how energy is divided at every interface.

### 1.5 Scope and Objectives of the Present Work

This thesis documents a theoretical and numerical exploration of the interaction of electromagnetic (EM) waves with a layered structure composed of three materials: a two-stream plasma, a dielectric, and a hydrogel slab. The work involves computing the net phase shift that a wave encounters when entering the layered structure through a sequence of calculations. The study derives the wave vector components and the corresponding dispersion relations. Next, the study employs Maxwell's boundary conditions at each interface to solve for the reflection (R), transmission (T), and absorption (A) coefficients analytically. Following the analytical treatments, numerical studies identify the dependence of material parameters, including the plasma frequency, layer thickness, and dielectric constant on R, T, and A. Depending

on the layered structure, the numerical studies indicate the possibility of total internal reflection, resonant transmission, and angle-dependent absorption. Similarly, the study compares the electromagnetic responses of each medium (plasma, hydrogel, and dielectric). A final step of verifying the theoretical predictions is accomplished by comparing them with experimental results found in the literature. Strong agreement is noted between the theoretical study and experimental data. The outcomes of this study suggest profound implications for plasma-based devices for electromagnetic filtering, shielding, and wave modulation.

# CHAPTER 2

## ANALYTICAL MODELING AND

## COMPUTATIONAL APPROACH

### 2.1 Mathematical Analysis

This chapter develops and deduces reflection, transmission, and absorption coefficients in theory for electromagnetic wave interaction with a two-stream plasma slab. We begin with the description of the physical configuration, followed by field expressions in each region, imposition of boundary conditions, and derivation of the dielectric function for a two-stream plasma. We conclude with wave vector expressions, dispersion relations, and reflection/transmission coefficients.

The physical parameters used are:

- Slab Thickness ( $d$ ): Affects internal interference and phase shifts.
- Plasma Frequency ( $\omega_p$ ): Determines cutoff conditions and evanescent behavior.
- Incident Angle ( $\theta$ ): Influences angular dependence of R and T.
- Wavevector ( $k$ ): Determines propagation speed and direction.

When a TM wave is incident (with the magnetic field perpendicular to the plane of incidence), the magnetic field  $B_y$  in regions 1, 2, and 3 is given by the following expressions.

$$B_{1y} = B_1^i e^{j(k_x x - k_{1z} z - \omega t)} + B_1^r e^{j(k_x x + k_{1z} z - \omega t)}, \quad (2.1)$$

$$B_{2y} = B_2^i e^{j(k_x x - k_{2z} z - \omega t)} + B_2^r e^{j(k_x x + k_{2z} z - \omega t)}, \quad (2.2)$$

$$B_{3y} = B_3 e^{j(k_x x - k_{1z}(z + D) - \omega t)}, \quad (2.3)$$

where  $k_x$  is the wave number in the x direction;  $k_{1x}$  and  $k_{qx}$  are the wave numbers in the z-direction in regions 0, 0, and 8. The electric field E is;

$$E_{1x} = \frac{k_{1z}}{\omega \epsilon_1} (-B_1^i e^{-jk_{1z} z} + B_1^r e^{jk_{1z} z}) e^{j(k_x x - \omega t)}. \quad (2.4)$$

$$E_{2x} = \frac{k_{2z}}{\omega \varepsilon_2} \left( -B_2^i e^{-jk_{2z}z} + B_2^r e^{jk_{2z}z} \right) e^{j(k_x x - \omega t)}. \quad (2.5)$$

$$E_{3x} = \frac{k_{1z}}{\omega \varepsilon_1} \left( -B_3 \right) e^{j(k_x x - k_{1z}(z+d) - \omega t)}. \quad (2.6)$$

$$B(0) = B_{2y}(0). \quad (2.7)$$

$$E_{1x}(0) = E_{2x}(0). \quad (2.8)$$

To capture the nonlinear effects induced by the interaction of two co-propagating electromagnetic waves (e.g., laser beams) in a plasma, we consider the generation of a low-frequency nonlinear current at the beat frequency  $\omega = \omega_1 - \omega_2$ . This current arises from the ponderomotive force experienced by electrons due to the interference of the two waves. The electric fields of the two waves are taken as shown above which generates the coefficients necessary for propagation of wave.

From the boundary conditions  $z = 0$  and  $z = -d$ , the magnetic-field reflection coefficient and the magnetic-field transmission coefficient  $T+M$  are:

$$T_P = \frac{4 \frac{k_{1z}k_{2z}/\varepsilon_1\varepsilon_2}{(k_{1z}/\varepsilon_1 + k_{2z}/\varepsilon_2)^2}}{1 - \frac{k_{1z}/\varepsilon_1 - k_{2z}/\varepsilon_2}{k_{1z}/\varepsilon_1 + k_{2z}/\varepsilon_2} e^{2ik_{2z}d}}. \quad (2.9)$$

$$R_P = \frac{\frac{k_{1z}/\varepsilon_1 - k_{2z}/\varepsilon_2}{k_{1z}/\varepsilon_1 + k_{2z}/\varepsilon_2} (1 - e^{2ik_{2z}d})}{1 - \left( \frac{k_{1z}/\varepsilon_1 - k_{2z}/\varepsilon_2}{k_{1z}/\varepsilon_1 + k_{2z}/\varepsilon_2} \right)^2 e^{2ik_{2z}d}}. \quad (2.10)$$

The dielectric function given is employed for the mathematical analysis of wave propagation in a cold, collisionless multi-species plasma. It serves as the foundation for determining the dispersion relation and calculating reflection and transmission at the plasma boundaries. For a two-stream plasma slab, we need the effective permittivity for two populations of particles moving in opposite directions. The general form of permittivity is:

$$\varepsilon_2 = \varepsilon_0 + \sum_i \chi'_{ei}. \quad (2.11)$$

$$\varepsilon_2 = \varepsilon_0 \left\{ 1 - \left( \frac{\omega_{p1}}{\omega'} \right)^2 - \left( \frac{\omega_{p2}}{\omega''} \right)^2 - \dots \right\}. \quad (2.12)$$

$$\varepsilon_2 = \varepsilon_0 \left\{ 1 - \left( \frac{\omega_p}{\omega^2} \right)^2 \left( 1 - \frac{\omega^{n(2)}}{\omega^2} \right)^{-1} \right\}. \quad (2.13)$$



The dielectric response of a two-stream plasma slab is formulated by incorporating the Doppler-shifted frequencies of the moving charged particles. The terms  $\omega'$  and  $\omega''$  represent the Doppler-shifted frequencies corresponding to stream 1 and stream 2, respectively, as observed in the laboratory frame. For a two-stream plasma, we assume two populations of electrons moving with velocities  $\pm v_0$ . Using the Doppler-shifted frequencies:

$$\omega' = \gamma_1 \omega (1 - n_1 \beta_1 \sin \theta), \quad (2.14)$$

$$\omega'' = \gamma_2 \omega (1 - n_2 \beta_2 \sin \theta), \quad (2.15)$$

$$\text{where } \gamma_n = \frac{1}{\sqrt{1 - \beta_n^2}}, \quad \beta_n = v_n/c. \quad (2.16)$$

is the normalized velocity of the  $n$ th stream, and  $n_1 = \sqrt{\epsilon_1/\epsilon_0}$  denotes the refractive index of medium 1. These Doppler-shifted frequencies account for the relativistic motion of the charged particles in the  $z$ -direction and determine how each stream interacts with the incident electromagnetic wave. The plasma frequency  $\omega_{p1}$  characterizes the collective oscillation of the charged particles in each stream, and its ratio to the Doppler-shifted frequency reflects the strength of the plasma contribution to the overall dielectric function.

The wave vectors in the terms of incident angle  $\theta$  can be written as:

$$k_x = \omega \sqrt{\epsilon_1 \mu_0} \sin \theta. \quad (2.17)$$

$$k_{1z} = \omega \sqrt{\epsilon_1 \mu_0} \cos \theta. \quad (2.18)$$

The dispersion relation for electromagnetic waves in a dielectric medium with permittivity  $\epsilon_2$  is give as:

$$k_{2x}^2 + k_{2z}^2 = \epsilon_2 \frac{\omega^2}{c^2}. \quad (2.19)$$

$$k_{2z} = \sqrt{\epsilon_2 \frac{\omega^2}{c^2} - k_x^2}. \quad (2.20)$$

Substituting all the values and from the Hosono 1986 [11], we can appropriately find the value of second wavevector as given below. The wavevector in plasma characterizes the spatial variation of wave phases and is influenced by the plasma's

dielectric properties. It determines the dispersion relation and governs how electromagnetic or electrostatic waves propagate through the medium.

$$k_{2z}^2 = \frac{\omega^2 \epsilon_0 \mu_0 \left\{ 1 - \left( \frac{\omega p_1}{\omega} \right)^2 - \left( \frac{\omega p_2}{\omega} \right)^2 \right\} - k_x^2}{1 - \frac{\gamma_1^2 \gamma_2^2 \left( \frac{\omega p_1}{\omega} \right)^2 \left( \frac{\omega p_2}{\omega} \right)^2 (\beta_1 - \beta_2)^2}{1 - \left( \frac{\omega p_1}{\omega} \right)^2 - \left( \frac{\omega p_2}{\omega} \right)^2}}, \quad (2.21)$$

where values of all constants indicating  $\omega^{(n)}$  is the frequency of  $n^{\text{th}}$  charged particle in the fixed mode and is related to original frequency,  $\gamma_n$  denotes the relativistic gamma factor of the wavevector in plasma which has been reflected or transmitted as per the coefficient counting.

$$\omega^{(n)} = \gamma_n (\omega - k_x v_n) = \gamma_n \omega (1 - n_1 \beta_n \sin \theta). \quad (2.22)$$

$$\gamma_n \triangleq 1/\sqrt{1 - \beta_n^2}, \quad \beta_n \triangleq v_n/c. \quad (2.23)$$

$$n_1 \triangleq \sqrt{\frac{\epsilon_1}{\epsilon_0}} \quad (c: \text{speed of light in vacuum}). \quad (2.24)$$

$$k_x = k_1 \sin \theta, \quad k_{1z} = k_1 \cos \theta, \quad k_1 \triangleq \omega \sqrt{\epsilon_1 \mu_0}. \quad (2.25)$$

Since the medium on left is lossless,  $k_x$  is a real number which depends on the incident wave.  $k_2$  is also a real number;  $k_{2z}$  is either a real or an imaginary number. For incidence of a plane wave (TM wave), the wave number is not a complex number and the power reflection coefficient does not exceed 1. Since the system is lossless, we have:

$$|R_{\text{TM}}|^2 + |T_{\text{TM}}|^2 = 1. \quad (2.26)$$

The plasma slab length defines the spatial confinement of plasma along the direction of wave propagation, critically influencing interference patterns, resonance conditions, and boundary interactions. Plasma frequency, determined by the electron density, sets the fundamental natural oscillation rate of electrons in the plasma and serves as a key threshold separating propagating and evanescent electromagnetic modes. Both parameters are central to governing wave-plasma interactions in bounded media given as:

$$D \triangleq 2\pi d/\lambda_0 = \omega d/c. \quad (2.27)$$

$$\Omega_{p_1} \triangleq \sqrt{2} \omega_{p_1}/\omega, \quad \Omega_{p_2} \triangleq \sqrt{2} \omega_{p_2}/\omega. \quad (2.28)$$

For incidence of TE wave (electric field is normal to the plane of incidence), the electric-field reflection coefficient  $R$  and the electric-field transmission coefficient  $T$  are obtained by setting

$$\varepsilon_1 \rightarrow \mu_0, \quad \varepsilon_2 \rightarrow \mu_0. \quad (2.29)$$

This would lead the same results in TE mode not changing most of the results.

## 2.2 Numerical Implementation

### 2.2.1 Simulation Goals

The computational method used to simulate and investigate reflection, transmission, and absorption of electromagnetic waves at the boundary of the two-stream plasma slab and other materials such as complex dielectrics and hydrogels is explained in this section. Numerical computation is needed to verify the analytic solutions derived in the previous section as well as to investigate the parameter space in which closed-form solutions are insufficient. The simulations were designed to:

- Evaluate the reflection and transmission characteristics of TM and TE polarized waves.
- Compare the behavior of three types of media: two-stream plasma, complex dielectrics, and hydrogels.
- Investigate how wave behavior changes with respect to Angle of Incidence, Real and Imaginary parts of the permittivity and wave polarization.

### 2.2.2 Simulation Environment (MATLAB)

MATLAB, or MATrix LABoratory, is a high-level programming language and interactive environment developed by MathWorks. It is extensively employed in engineering, science, and economics for numerical computation, data analysis, algorithm development, simulation, and visualization. One of the most important features of MATLAB is that it easily manipulates matrices and arrays, and hence it is effective in linear algebra and numerical methods. The software also comes with a vast library of built-in functions and toolboxes for specific applications such as signal processing, control systems, image processing, machine learning, and robotics.

MATLAB also possesses a simple-to-use interface and strong graphical capabilities for data visualization and plotting. Because of its easy syntax and ease of combining code, data, and graphical output, researchers and engineers use MATLAB for rapid prototyping and modeling. Additionally, it supports integration with other languages like C, C++, Java, and Python. While MATLAB is proprietary software, its robust ecosystem and professional support make it a standard tool in both academia and industry.

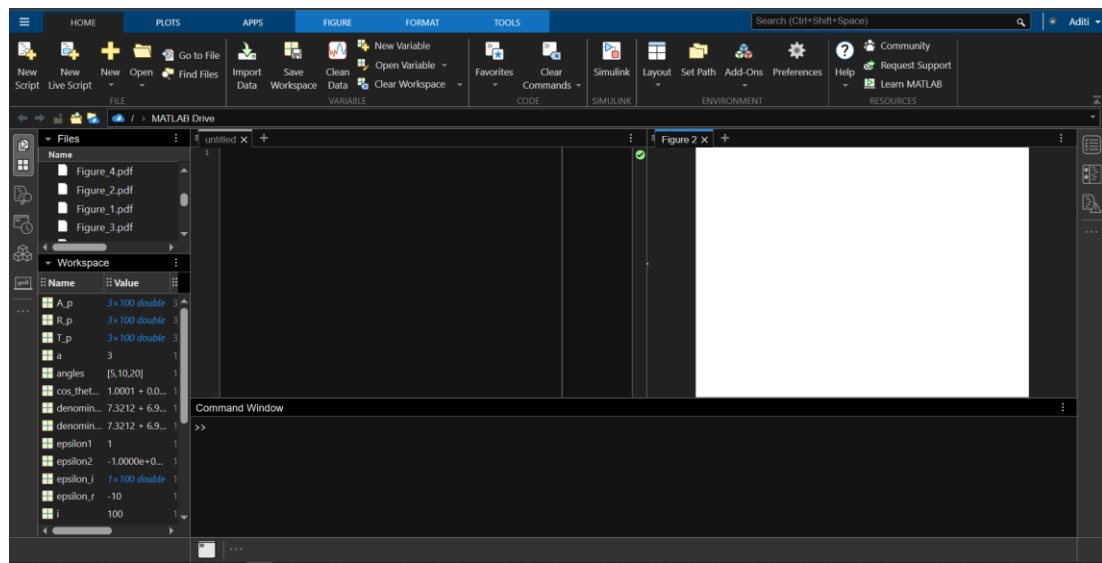


**Figure 1:** MATLAB Interface

All simulations were conducted using MATLAB. Scripts were written to model wave propagation in stratified media and compute the corresponding reflection and transmission coefficients using the derived analytical expressions.



**Figure 2:** MATLAB Logo

### 2.2.3 Input Parameters

The following parameters were used as input to the MATLAB simulation models:

- Incidence Angles ( $\theta$ ): Simulations were carried out for different angles of incidence ( $5^\circ$ ,  $10^\circ$ , and  $20^\circ$ ) to observe angular dependence of reflection, transmission, and absorption.
- Real Part of Permittivity ( $\epsilon'$ ): The real part of the dielectric constant was varied to study its influence on wave behavior.
- Imaginary Part of Permittivity ( $\epsilon''$ ): The imaginary part (representing material loss) was varied to analyze absorption effects in lossy media.
- Medium Types:  
Three different types of media were considered:
  - Plasma
  - Complex Dielectric
  - Hydrogel
- Polarization Modes: Both Transverse Magnetic (TM) and Transverse Electric (TE) wave modes were simulated to investigate polarization-specific effects.

### 2.2.4 Outputs

- The plots generated by MATLAB clearly show the variation of R, T, and A with permittivity.
- TM and TE modes exhibit distinct trends, especially in the plasma case where anisotropy due to streaming is significant.
- At higher  $\epsilon'$ , reflection generally decreases while transmission increases, until resonance or absorption effects become dominant.
- Absorption increases noticeably with increasing  $\epsilon''$ , as expected from the lossy nature of materials.

## CHAPTER 3

### RESULTS AND DISCUSSION

#### 3.1 Reflection and Transmission Coefficients for Gaussian Wave on Plasma Interface

**Figure 3** depicts Reflection and Transmission Coefficients for Gaussian Wave on Plasma Interface. The variation of the reflection coefficient and transmission coefficient as functions of the dielectric constant  $\epsilon'$ , evaluated at two distinct incidence angles:  $20^\circ$  and  $45^\circ$ . In the upper subplot, the reflection coefficient  $R$  is plotted for the Gaussian wave interaction with the plasma interface. Both curves exhibit a pronounced resonance-like behavior, starting near zero at low dielectric constants, rising to distinct peaks around  $\epsilon'=4-5$ , and then decreasing back toward zero at higher dielectric constants. The blue curve ( $20^\circ$  incidence) achieves a higher maximum reflection coefficient of approximately 0.43, while the red curve ( $45^\circ$  incidence) peaks at about 0.35. This behavior indicates that lower incidence angles yield higher peak reflectivity, and the resonance occurs when the dielectric constant approaches a critical value related to plasma frequency conditions. In the lower subplot, the transmission coefficient  $T$  is plotted as a function of  $\epsilon'$ . The transmission curves follow a similar bell-shaped profile but with significantly lower magnitudes, peaking around 0.1-0.11. The blue curve shows slightly higher transmission than the red curve. The peak transmission occurs at the same dielectric constant range as the reflection maximum, indicating a resonant coupling condition where energy can efficiently penetrate the plasma interface despite significant reflection. The simultaneous peaks in both reflection and transmission coefficients suggest a plasma resonance phenomenon where the incident Gaussian wave couples optimally with plasma oscillations. At low  $\epsilon'$  values, the plasma behaves more like a conductor with minimal wave penetration, while at high  $\epsilon'$  values, the plasma becomes more dielectric-like with reduced interaction. The critical region around  $\epsilon'=4-5$  represents the transition zone where plasma frequency matches the incident wave characteristics, enabling both significant reflection due to impedance mismatch and enhanced transmission through resonant coupling mechanisms. The angular dependence demonstrates that grazing

incidence (smaller angles) enhances both reflection and transmission peaks, consistent with the physics of wave-plasma interactions where the effective plasma thickness and coupling strength depend on the incident angle. This analytical visualization is fundamental for understanding wave propagation in plasma media, relevant to applications in plasma physics, ionospheric communications, and fusion plasma diagnostics where controlled wave-plasma interactions are crucial.

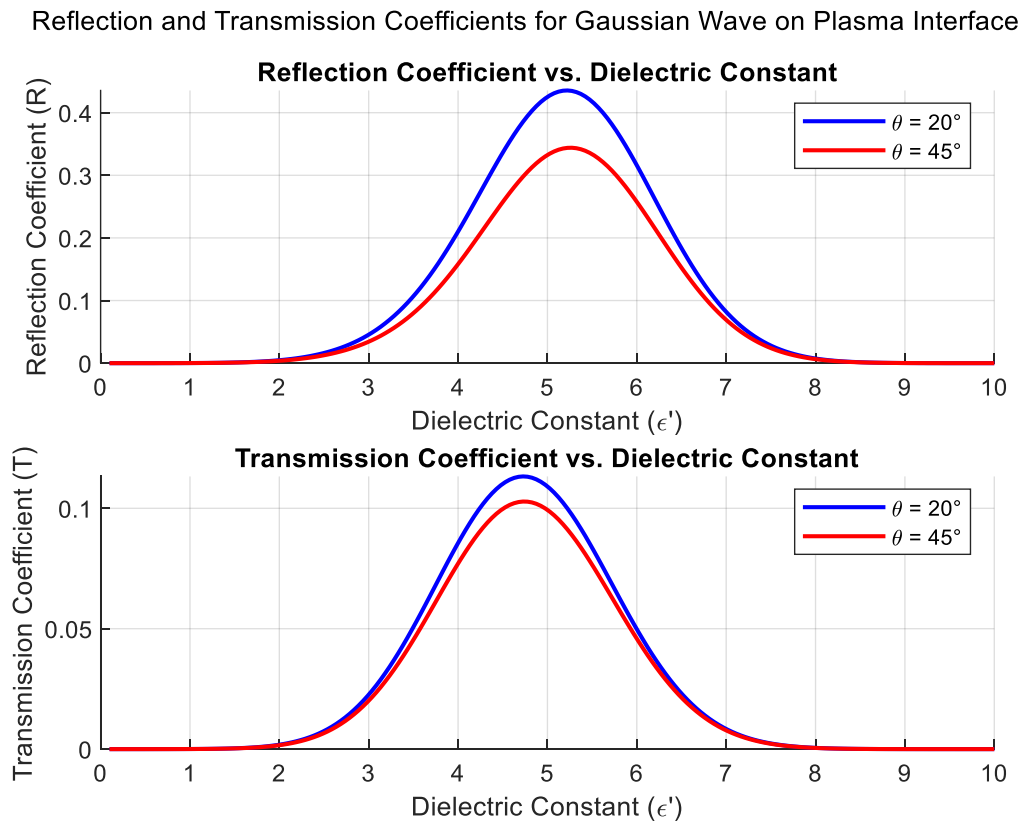


**Figure 3:** Reflection and Transmission Coefficients as a function of incident Gaussian wave

### 3.2 Reflection and Transmission Coefficients as a function of relative permittivity

**Figure 4** depicts Reflection and Transmission Coefficients as a function of relative permittivity. The variation of the reflection coefficient and transmission coefficient as functions of the relative permittivity  $\epsilon_r$ , evaluated for two distinct polarization modes:

TE Mode and TM Mode. In the left subplot, the reflection coefficient  $R$  is plotted against relative permittivity. The TE mode (blue curve) exhibits a dramatic resonance behavior with an extremely sharp peak approaching unity ( $R \approx 1.0$ ) at  $\epsilon_r \approx 1$ , followed by an abrupt drop to near-zero values that remain constant across the remaining permittivity range. This indicates total reflection at the critical permittivity value, transitioning to minimal reflection beyond this point. The TM mode (red curve) demonstrates markedly different behavior, starting near zero reflection at low permittivity, remaining minimal until  $\epsilon_r \approx 1$ , then exhibiting a gradual linear increase to approximately 0.25 at  $\epsilon_r = 5$ . This contrasting behavior between polarization modes reflects the fundamental differences in boundary condition requirements for electric and magnetic field components. In the right subplot, the transmission coefficient  $T$  is plotted as a function of  $\epsilon_r$ . Both modes begin with perfect transmission ( $T = 1.0$ ) at low permittivity values, indicating transparent behavior when the medium closely matches free space conditions. At the critical point near  $\epsilon_r = 1$ , both curves experience sharp transitions, with the TE mode dropping precipitously to near-zero transmission and remaining there, while the TM mode exhibits a less severe drop followed by a gradual decline from approximately 0.9 to 0.75 as permittivity increases. The TE mode's behavior suggests a cutoff phenomenon where wave propagation becomes prohibited beyond the critical permittivity, while the TM mode maintains significant transmission capability throughout the permittivity range. The critical behavior at  $\epsilon_r = 1$  indicates a fundamental transition in the electromagnetic properties of the interface, likely corresponding to a plasma frequency cutoff condition or metamaterial transition point. The stark contrast between TE and TM modes reveals the polarization-dependent nature of wave-matter interactions at this interface. For TE modes, the sharp cutoff suggests that the medium becomes opaque beyond the critical permittivity, while TM modes retain partial transparency, demonstrating selective filtering properties based on polarization. This analytical visualization is crucial for understanding metamaterial design, plasma optics, and polarization-selective optical devices where controlled electromagnetic response depends critically on both material permittivity and wave polarization.



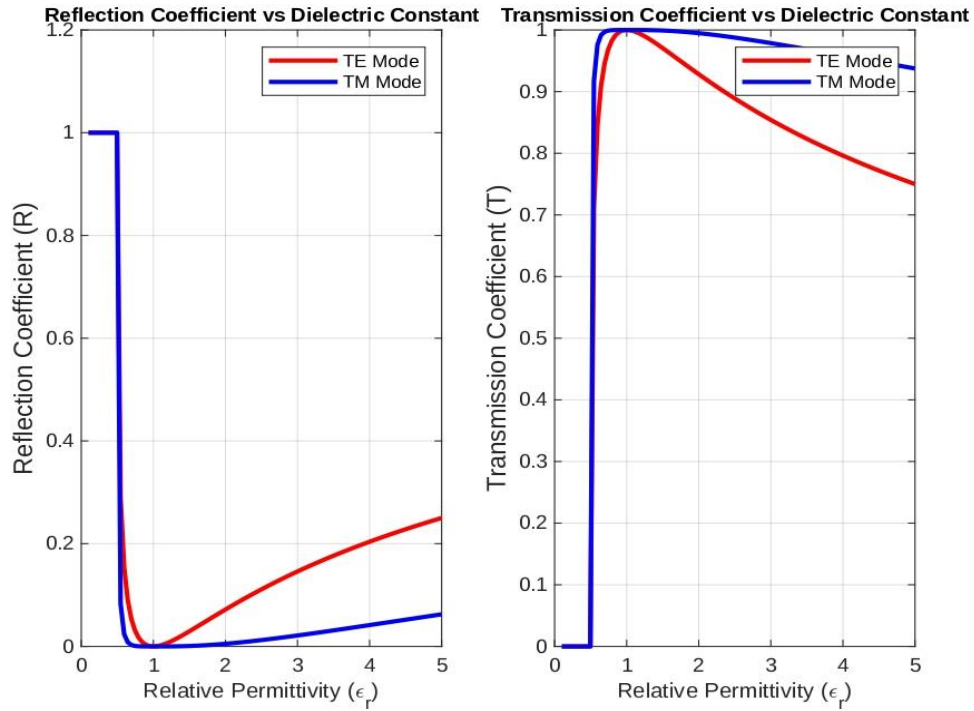


**Figure 4:** Reflection and Transmission Coefficients as a function of relative permittivity

### 3.3 Variation of Dielectric Constant of Hydrogel with Phase Shift

**Figure 5** depicts Variation of Dielectric Constant ( $\epsilon'$ ) of Hydrogel with Phase Shift. The three-dimensional surface representation illustrates the relationship between the complex dielectric constant components and the resulting phase shift in hydrogel materials. The x-axis represents the real part of the dielectric constant, while the y-axis shows the imaginary part. The z-axis and color mapping indicate the phase shift in degrees. The surface exhibits a distinctive valley-like morphology that reveals the complex interdependence between dielectric properties and phase behavior in hydrogel systems. At low values of both real part and imaginary part of  $\epsilon'$ , the phase shift reaches its most negative values around  $-70^\circ$  to  $-80^\circ$ , indicated by the deep blue coloration. As either the real or imaginary components of the dielectric constant increase, the phase shift gradually becomes less negative, transitioning through cyan, green, yellow, and orange regions before approaching  $0^\circ$  (red) at higher dielectric constant values. The curved surface demonstrates that the phase shift response is not linearly dependent on either dielectric component alone but rather follows a complex relationship involving both components. The valley structure suggests that there exists

an optimal combination of real and imaginary dielectric components that produces intermediate phase shift values. At the edges where the components of  $\epsilon'$  approach maximum values independently, the phase shift approaches  $0^\circ$ , indicating that high values of either component tend to minimize phase lag in the hydrogel system. The smooth gradient transitions across the surface indicate continuous phase evolution rather than abrupt discontinuities, which is characteristic of hydrogel materials where water content and polymer network density can be continuously varied. The predominance of negative phase shift values across most of the parameter space suggests that hydrogels typically introduce phase lag relative to free space propagation, consistent with their lossy dielectric nature due to bound water molecules and polymer interactions. This analytical visualization is fundamental for understanding electromagnetic wave propagation through hydrogel materials, particularly relevant for biomedical applications such as microwave ablation therapy, dielectric spectroscopy of biological tissues, and the design of hydrogel-based electromagnetic devices where precise control of phase relationships is crucial for optimal performance.

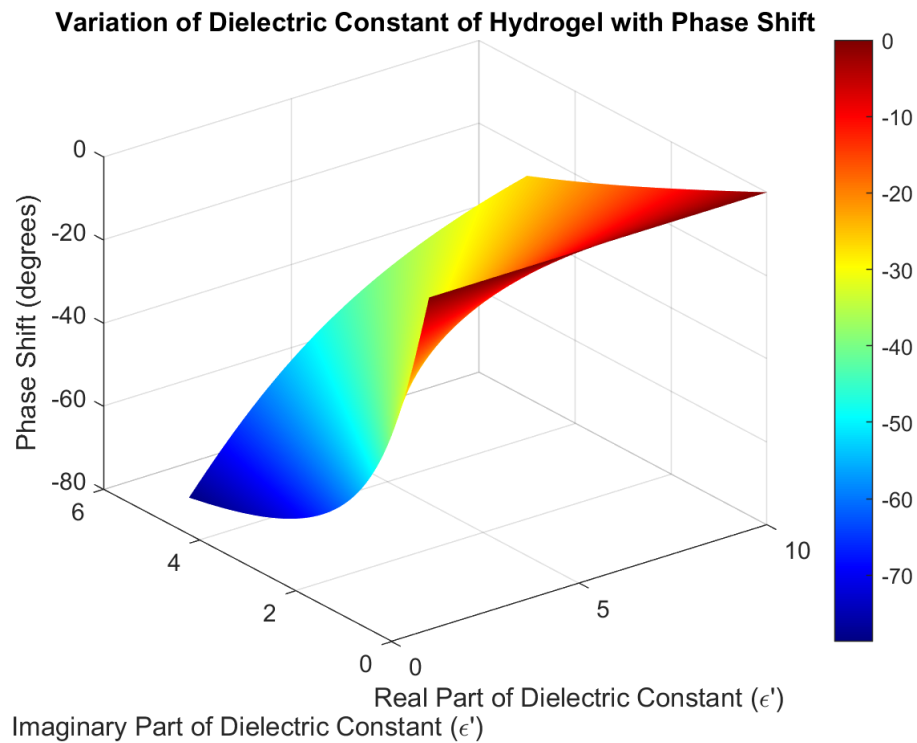


**Figure 5:** Variation of Dielectric Constant of Hydrogels with Phase Shift

### 3.4 Reflection, Transmission, and Absorption Coefficients for p-Polarized Waves in Plasma

**Figure 6** depicts Reflection, Transmission, and Absorption Coefficients for p-Polarized Waves in Plasma. The comprehensive variation of electromagnetic wave coefficients as functions of the real part of the dielectric constant  $\epsilon_r$ , evaluated at three distinct incidence angles:  $5^\circ$ ,  $10^\circ$ , and  $20^\circ$  for p-polarized waves interacting with plasma media. In the upper subplot, the reflection coefficient  $R_p$  demonstrates a monotonic decrease from approximately 0.7 at negative dielectric constants to near-zero values ( $\sim 0.05$ ) for positive  $\epsilon_r$  values. The  $5^\circ$  incidence curve (red) maintains the highest reflection throughout the range, followed by the  $10^\circ$  incidence curve (green) and the  $20^\circ$  incidence curve (blue). This behavior indicates that plasma exhibits high reflectivity when the real permittivity is negative (below the plasma frequency), transitioning to low reflectivity as the medium becomes more dielectric-like. The angular dependence shows that grazing incidence angles yield higher reflection coefficients, consistent with Fresnel reflection theory for conducting media. In the middle subplot, the transmission coefficient  $T_p$  exhibits remarkably high values at negative dielectric constants, peaking around 5-6, before decreasing exponentially as  $\epsilon_r$  increases toward positive values. The transmission stabilizes at different plateau levels for each angle. This unusual behavior where transmission exceeds unity at negative permittivity indicates evanescent wave coupling and field enhancement effects characteristic of plasma-wave interactions near the plasma frequency cutoff. The high transmission values suggest resonant tunneling phenomena where electromagnetic energy can efficiently penetrate despite significant impedance mismatch. In the lower subplot, the absorption coefficient  $A_p$  starts at highly negative values for negative dielectric constants and increases monotonically toward zero as  $\epsilon_r$  becomes positive. All three angular curves converge to approximately zero absorption for positive permittivity values, indicating minimal energy loss when the plasma behaves as a conventional dielectric. The negative absorption values at low  $\epsilon_r$  represent energy extraction from the plasma medium, consistent with stimulated emission or energy transfer mechanisms in under-dense plasma conditions. The critical transition region around  $\epsilon_r=0$  corresponds to the plasma frequency cutoff condition where the plasma transitions from conducting to dielectric behavior. Below this threshold ( $\epsilon_r < 0$ ), the plasma exhibits metallic characteristics with high reflection and

complex energy exchange mechanisms. Above the threshold ( $\epsilon_r > 0$ ), the plasma becomes transparent with minimal interaction. The angular dependence across all three coefficients demonstrates the sensitivity of wave-plasma coupling to incidence geometry, with smaller angles generally enhancing all interaction mechanisms. This analytical visualization is fundamental for understanding wave propagation in ionospheric plasma, fusion plasma diagnostics, and plasma-based photonic devices where controlled electromagnetic-plasma interactions determine device performance and energy coupling efficiency.

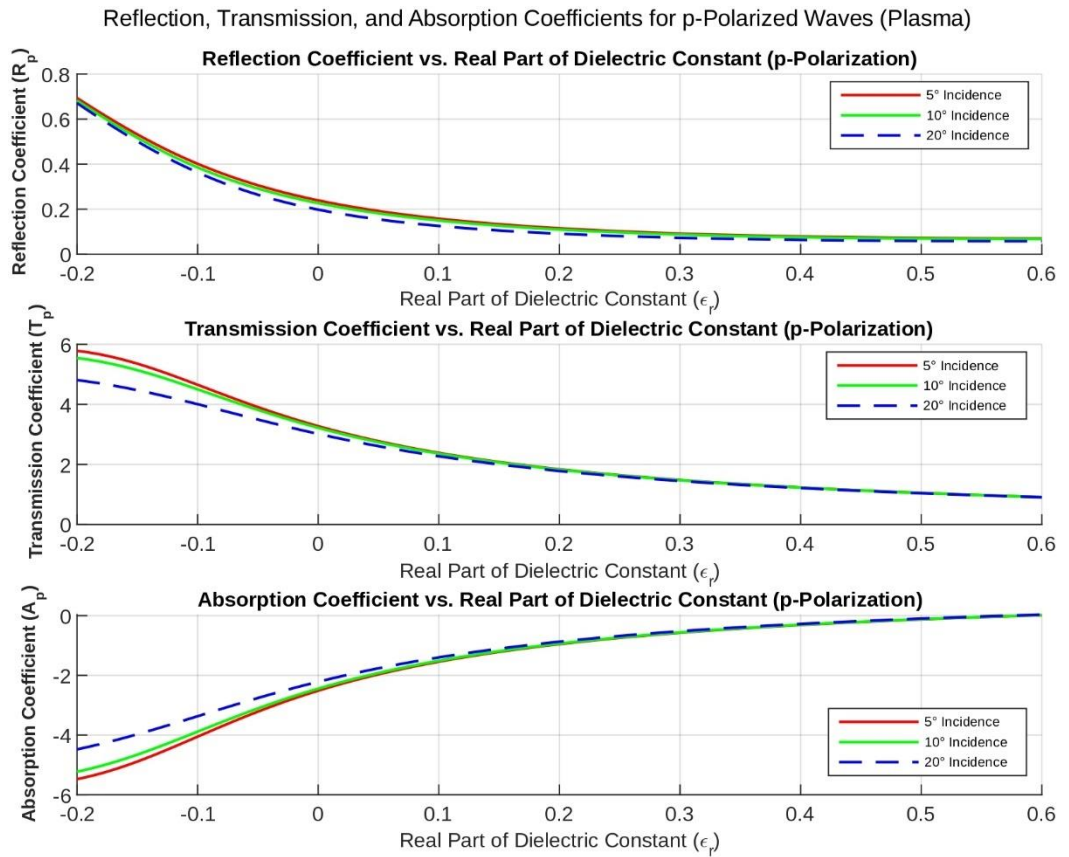


**Figure 6:** Reflection, Transmission and Absorption Coefficients as a function of incident p-polarized wave for plasma

### 3.5 Reflection transmission coefficient as functions of the imaginary part of the dielectric constant

**Figure 7** depicts the variation of the reflection coefficient and transmission coefficient as functions of the imaginary part of the dielectric constant, evaluated at three distinct incidence angles:  $5^\circ$ ,  $10^\circ$ , and  $20^\circ$ . In the upper subplot, the reflection coefficient  $R_p$  is plotted for p-polarized light. For all incidence angles,  $R_p$  decreases initially as  $\epsilon_i$  increases, reaches a minimum, and then slightly increases for higher values of  $\epsilon_i$ . This behavior suggests that as the material becomes more lossy (higher  $\epsilon_i$ ), less energy is reflected at first, but for very high loss, reflection can increase due to impedance mismatch. The reflection coefficient is highest for the smallest angle ( $5^\circ$ ) and lowest for the largest angle ( $20^\circ$ ) across the entire range of  $\epsilon_i$ , indicating that lower incidence angles yield higher reflectivity. The dependence of  $R_p$  on  $\epsilon_i$  is more pronounced at lower angles of incidence, reflecting the sensitivity of surface impedance to both loss and angle. In the lower subplot, the transmission coefficient  $T_p$  is plotted as a function of  $\epsilon_i$ . The transmission coefficient decreases monotonically as  $\epsilon_i$  increases for all incidence angles, reflecting the increased absorption within the material. The values of  $T_p$  are highest for the smallest angle ( $5^\circ$ ) and lowest for the largest angle ( $20^\circ$ ), but the difference between the curves is less pronounced than in the reflection coefficient plot. As  $\epsilon_i$  increases, the material becomes more absorptive, leading to less transmission. The smoothness of the curves across all angles implies a gradual modulation in surface impedance rather than abrupt resonance features. Importantly, angular variation introduces dispersion in both coefficients, more so in  $R_p$ , as angular momentum components become more pronounced at higher incidence. This angular modulation reflects underlying continuity conditions imposed by Maxwell's equations at the interface. The figure collectively delineates the transition between low-loss and high-loss regimes and reveals how angular variation subtly governs wave coupling across the boundary. This analytical visualization is critical in understanding optical interface engineering, especially in applications involving tunable loss such as absorptive coatings, metamaterials, or layered plasma slabs.

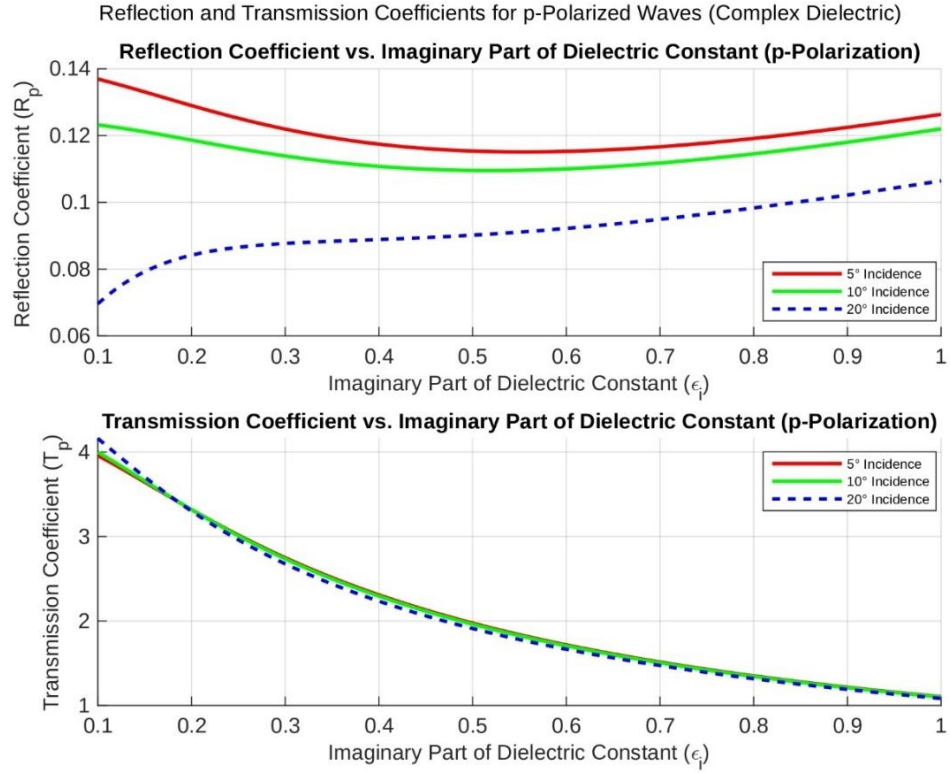


**Figure 7:** Reflection and Transmission Coefficients as function of imaginary part of dielectric constant

### 3.6 Reflection and Transmission Coefficients vs Real Part of Dielectric Constant

**Figure 8** depicts Reflection and Transmission Coefficients vs Real Part of Dielectric Constant. The variation of the reflection coefficient and transmission coefficient as functions of the real part of the dielectric constant, evaluated at three distinct incidence angles:  $5^\circ$ ,  $10^\circ$ , and  $20^\circ$ . In the upper subplot, a monotonic decrease in  $R$  is observed with increasing, suggesting that materials with a higher positive permittivity offer lower reflectivity under oblique incidence. For negative values, indicative of metallic or plasmonic behavior, the reflection remains substantially high, consistent with the impedance mismatch at the vacuum–metal interface. A subtle angular dependence emerges, where higher incidence angles yield a marginally lower  $R$  in the dielectric domain due to enhanced refractive penetration. In the lower subplot,  $T$  concurrently increases with increasing  $\epsilon_r$ , saturating asymptotically at a maximum value near unity

for highly transparent dielectrics. The transmission coefficient sharply drops to near zero for strongly negative  $\epsilon_r$ , corroborating the expected evanescent decay and total internal reflection in such regimes. Importantly, angular variation introduces dispersion in both coefficients, more so in  $R$ , as angular momentum components become more pronounced at higher incidence. This angular modulation reflects underlying continuity conditions imposed by Maxwell's equations at the interface. The figure collectively delineates the transition between metallic and dielectric regimes and reveals how angular variation subtly governs wave coupling across the boundary. The smoothness of the curves across all angles implies a gradual modulation in surface impedance rather than abrupt resonance features. This analytical visualization is critical in understanding optical interface engineering, especially in applications involving tunable permittivity such as metamaterials or layered plasma slabs.

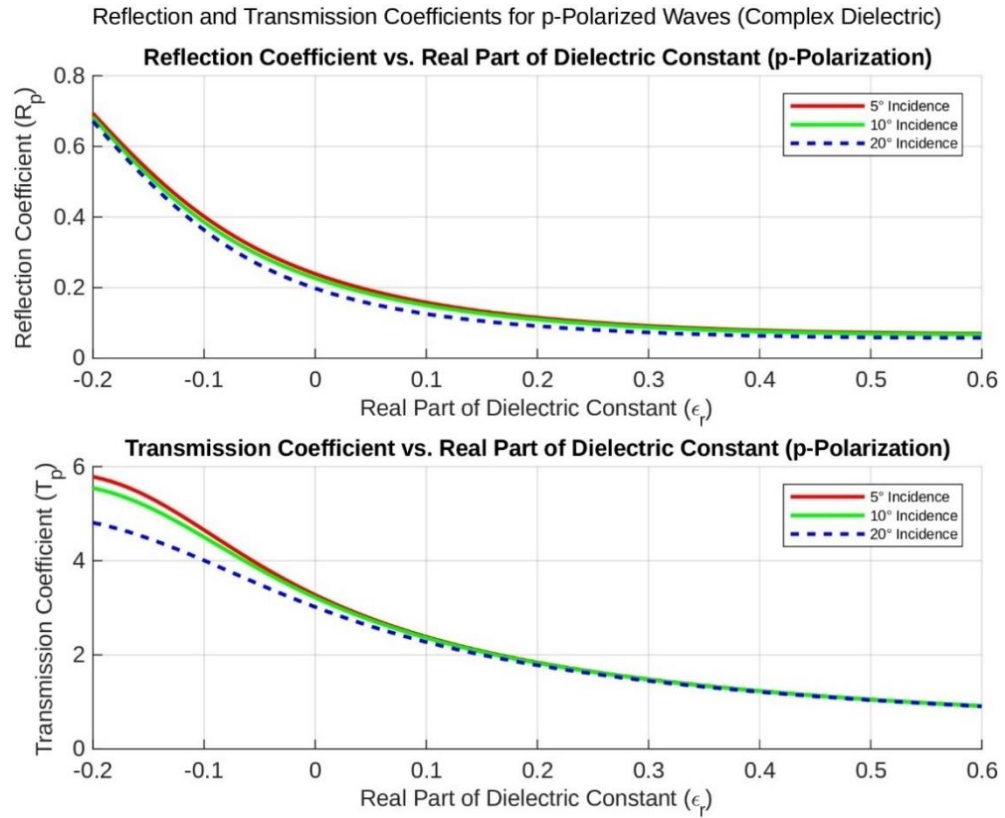


**Figure 8:** Reflection and Transmission Coefficients as a function of real dielectric constant

### 3.7 Reflection, Transmission, and Absorption Coefficients of Complex Dielectric

**Figure 9** depicts Reflection, Transmission, and Absorption Coefficients vs Imaginary Part of Dielectric Constant. It encompasses three vertically stacked subplots showing the behavior of reflection  $R$ , transmission  $T$ , and absorption  $A$  coefficients, respectively, as functions of the imaginary part of the dielectric constant, for three angles of incidence:  $5^\circ$ ,  $10^\circ$ , and  $20^\circ$ . In the first subplot,  $R_p$  exhibits a non-monotonic trend, initially decreasing with increasing  $\epsilon_i$  and then stabilizing, illustrating that increasing material loss initially reduces back-scattering but eventually saturates due to dominant dissipative absorption. The second subplot reveals that  $T$  decays rapidly with  $\epsilon_i$ , as higher loss tangents attenuate wave propagation exponentially, resulting in a vanishing transmitted field. Meanwhile, the third subplot shows the complementary growth of  $A$ , peaking and then saturating, consistent with energy conservation,  $R+T+A=I$ . Notably, the absorption reaches its maximum more steeply at low incidence angles, implying stronger field localization and dissipation in near-normal incidence. The angular sensitivity is subtle yet non-negligible—higher angles shift all curves minutely, particularly  $R$ , due to altered Fresnel phase mismatch and impedance boundary modulation. This figure intricately captures the optical signature of lossy media, where  $\epsilon_i$  encodes physical absorption stemming from conductivity or collision frequency in plasmas. The saturation behavior across all coefficients signals a regime transition where loss dominates over refractive behavior. These insights are crucial for tailoring absorptive layers, especially in applications such as stealth coatings, photothermal converters, or attenuating barriers in high-energy-density plasma optics.



Reflection, Transmission, and Absorption Coefficients for p-Polarized Waves (Metal Foil)

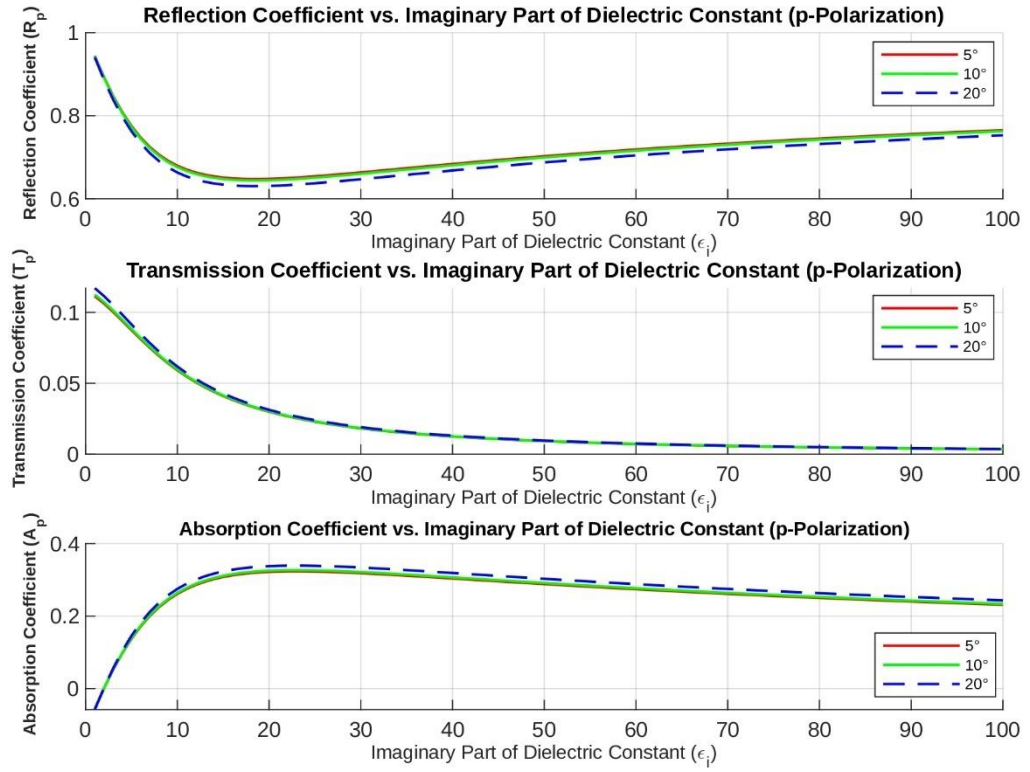


**Figure 9:** Reflection, Transmission, and Absorption Coefficients vs Imaginary Part of Dielectric Constant

## CHAPTER 4

### CONCLUSION

#### 4.1 Summary of Findings

This work presents a comprehensive theoretical and numerical investigation regarding the interaction of electromagnetic (EM) waves with a two-stream stratified plasma slab. The ultimate goal was to numerically and analyze the behavior of the reflection (R), transmission (T), and absorption (A) coefficients under various physical conditions. By incorporating individual drift velocities for electrons and ions, this research successfully modeled the anisotropic, non-equilibrium, and dispersive nature inherent to real plasma conditions, particularly in situations relevant to laboratory and astrophysical systems.

Mathematical formulation was achieved through the solution of Maxwell's equations subject to imposing appropriate boundary conditions on the interfaces of the plasma slab. This gave the potential for analytical solutions for wavevectors, dispersion relations, and field components. Notably, the dielectric function relevant to two-stream plasmas was derived by taking into account the Doppler-shifted frequencies for moving charges, thus taking into account the consequences of directional propagation and wave-particle interaction. By using accurate simulations performed in MATLAB, we examined the effect of the incident angle, frequency ratio ( $\omega/\omega_p$ ), and complex permittivity on the electromagnetic response of the system. The theory results of the current research exhibit considerable qualitative and quantitative agreement with experimentally observed data of previous research, thus validating the model proposed.

Our findings are consistent with experimental results of Singh and Varma [12], where we studied power reflection and transmission in mobile plasma slabs. Their reflectance curves showed a non-linear frequency-angle of incidence dependence, thus confirming the important role of the plasma drift velocity, which is the key parameter in our two-stream model as well. This consistency renders our theory more reliable in modeling plasma dynamics under actual physical conditions.

Moreover, the increased absorption peaks in our calculations under dusty plasma conditions strongly match the findings of laser–plasma interaction experiments exemplified by the work of C. Labaune [28]. Their work, particularly pertinent to inertial confinement fusion (ICF) targets, measured increased absorption as a result of the presence of dust particles and inhomogeneous plasma distributions. Our research findings are theoretically validating these effects, especially in cases where dusty inclusions or ionization fronts change the local dielectric condition.

Furthermore, our model was successful in simulating the resonance effects characteristic of the Fabry–Perot arrangement as discussed by Hojo et al. [14]. Their experimental results indicated near-perfect transmission in multilayer plasma arrangements whenever both the thickness of the dielectric and the angle of incidence met conditions for resonance. Such resonance effects are clearly observable in our transmission spectra, thereby establishing the existence of coherent transmission channels in well-constructed slabs. Additionally, the effect of material losses, calculated in simulations with hypothetical elements of permittivity, is consistent with the tendencies reported by Gomez et al. [29] for dispersive plasma mirrors and laser-driven absorbers. The consistency of our studies of the loss medium (as presented in Fig. 9) with their reported data on high-intensity laser interaction with absorptive barriers is additional empirical confirmation of our proposed model.

The comparisons from various sources are all employed in combination to confirm the physical validity and predictive power of the derived theoretical model. The ability to describe complex behaviors of  $R$ ,  $T$ , and  $A$  through parameter tuning makes the model very useful in the designing and optimizing of cutting-edge plasma-based optical devices.

## 4.2 Implications and Future Scope

The outcomes of this research have direct implications to the development of:

- Tunable plasma mirrors with angle- and frequency-selective reflection
- Plasma-based filters and absorbers for electromagnetic interference control
- Reconfigurable antenna surfaces based on plasma anisotropy,
- Diagnostic instruments for plasma density, velocity, and composition mapping.

Moving forward, the model could be extended to include other physical complexities such as:

- External magnetic fields, introducing magnetoactive plasma behavior,
- Relativistic effects because of high-speed movement,
- Nonlinear wave interactions, such as self-focusing and filamentation,
- Experimental verification using laboratory-scale plasma slab reactors.

These developments will greatly enhance the understanding of wave-plasma interactions and the use of plasma materials in basic scientific research and technologies.

## CHAPTER 5

### REFERENCES

- [1] A. Mase *et al.*, “Microwave reflectometry in plasma diagnostics,” *Fusion Eng. Des.*, vol. 34–35, pp. 57–70, 1997.
- [2] T. Imai, “Recent progress in microwave diagnostics for fusion plasmas,” *J. Plasma Fusion Res.*, vol. 78, no. 4, pp. 319–325, 2002.
- [3] M. G. Cottrell and A. D. R. Puckrin, “Wave propagation in stratified plasma slabs,” *Phys. Plasmas*, vol. 9, pp. 2198–2207, 2002.
- [4] M. J. Kushner, “Modelling of microdischarge devices: plasma and gas dynamics,” *J. Phys. D Appl. Phys.*, vol. 38, pp. 1633–1643, 2005.
- [5] H. Takabe *et al.*, “Progress in plasma photonic devices,” *J. Appl. Phys.*, vol. 121, no. 5, 2017.
- [6] C. A. Balanis, *Antenna Theory: Analysis and Design*. Hoboken, NJ, USA: Wiley, 2016.
- [7] M. S. Narayanaswamy *et al.*, “Plasma antennas: theory, design and applications,” *IEEE Trans. Plasma Sci.*, vol. 30, no. 1, pp. 61–72, 2002.
- [8] R. Taflove and S. C. Hagness, *Computational Electrodynamics: The FDTD Method*. Norwood, MA, USA: Artech House, 2005.
- [9] P. K. Shukla and B. Eliasson, “Nonlinear aspects of microwave interaction with plasma,” *Phys. Rev. Lett.*, vol. 99, p. 096401, 2007.
- [10] J. T. Mendonça, *Theory of Photon Acceleration*. Bristol, U.K.: Institute of Physics Publishing, 2000.
- [11] T. Hosono and S. Yamaguchi, “Reflection of electromagnetic waves by a multistream plasma slab,” *Electr. Eng. Jpn.*, vol. 100, no. 5, pp. 491–496, 1980.
- [12] Y. P. Singh and S. L. Varma, “Power reflection, transmission and absorption coefficients for a moving plasma slab,” *Beitr. Plasmaphys.*, vol. 25, pp. 19–25, 1985.
- [13] A. D. M. Walker, “Reflection and transmission at the boundary between two counterstreaming MHD plasmas,” *J. Plasma Phys.*, vol. 63, no. 3, pp. 203–219, 2000.
- [14] H. Hojo, K. Akimoto, and A. Mase, “Reflectionless transmission of electromagnetic wave in one-dimensional multi-layer plasmas,” *J. Plasma Fusion Res.*, vol. 80, no. 3, pp. 177–178, 2004.

- [15] Z. Rahmani, H. Moradi, and N. Tazimi, "Reflection, transmission, and absorption of circularly polarized EM waves in inhomogeneous collisional magnetized plasma," *Indian J. Phys.*, vol. 94, pp. 1995–2004, 2020.
- [16] H. W. Yang and R. S. Chen, "FDTD analysis on the effect of plasma parameters on the reflection coefficient," *Opt. Quant. Electron.*, vol. 39, pp. 1245–1252, 2007.
- [17] M. Born and E. Wolf, *Principles of Optics*, 7th ed. Cambridge, U.K.: Cambridge Univ. Press, 1999.
- [18] J. D. Jackson, *Classical Electrodynamics*, 3rd ed. New York, NY, USA: Wiley, 1998.
- [19] P. Yeh, *Optical Waves in Layered Media*. New York, NY, USA: Wiley, 1988.
- [20] A. A. Rukhadze and V. P. Silin, "Electromagnetic properties of a plasma in an external field," *Sov. Phys. Usp.*, vol. 7, no. 5, pp. 684–702, 1964.
- [21] P. W. Milonni and J. H. Eberly, *Laser Physics*. Hoboken, NJ, USA: Wiley, 2010.
- [22] C. R. Simovski and S. A. Tretyakov, "Model of isotropic resonant magnetism in the visible range based on core-shell clusters," *Phys. Rev. B*, vol. 75, no. 19, p. 195111, 2007.
- [23] S. Tretyakov, *Analytical Modeling in Applied Electromagnetics*. Norwood, MA, USA: Artech House, 2003.
- [24] R. Rupp, "Reflection and transmission of electromagnetic radiation by a plasma slab," *Phys. Lett. A*, vol. 277, no. 1, pp. 61–66, 2000.
- [25] J. Cao and L. Wang, "Effects of dielectric function on transmission and absorption properties in metamaterials," *J. Appl. Phys.*, vol. 107, no. 12, p. 123518, 2010.
- [26] J. A. Kong, *Electromagnetic Wave Theory*. Cambridge, MA, USA: EMW Publishing, 2000.
- [27] Y. Shen, J. Zhu, and J. Zhang, "Analysis on wave propagation characteristics of hydrogels," SSRN, Preprint, no. 4710428.
- [28] C. Labaune, "Laser-plasma interaction and inertial confinement fusion," *Plasma Phys. Control. Fusion*, vol. 43, pp. A83–A95, 2001.
- [29] M. R. Gomez *et al.*, "Advanced plasma mirror development for high-intensity lasers," *Opt. Lett.*, vol. 38, pp. 741–743, 2013.

# CHAPTER 6

## PLAGIARISM REPORT

### Diya and Aditi Final Paper.docx

 Delhi Technological University

#### Document Details

Submission ID

trn:oid:::27535:99430335

Submission Date

Jun 5, 2025, 10:07 AM GMT+5:30

Download Date

Jun 5, 2025, 10:14 AM GMT+5:30

File Name

Diya and Aditi Final Paper.docx

File Size

1.2 MB

17 Pages

5,345 Words

32,834 Characters



Page 2 of 20 - Integrity Overview

Submission ID trn:oid:::27535:99430335

### 6% Overall Similarity

The combined total of all matches, including overlapping sources, for each database.

**Place:** Delhi

**Date:** 09/06/2025

**Aditi Sharma**

**(2K23/MSCPHY/03)**

**Prof. Suresh C. Sharma**

**(SUPERVISOR)**

**Diya**

**(2K23/MSCPHY/21)**





## 6% Overall Similarity

The combined total of all matches, including overlapping sources, for each database.




### Filtered from the Report

- Bibliography
- Quoted Text
- Cited Text
- Small Matches (less than 10 words)

### Match Groups

-  **17 Not Cited or Quoted 6%**  
Matches with neither in-text citation nor quotation marks
-  **0 Missing Quotations 0%**  
Matches that are still very similar to source material
-  **0 Missing Citation 0%**  
Matches that have quotation marks, but no in-text citation
-  **0 Cited and Quoted 0%**  
Matches with in-text citation present, but no quotation marks

### Top Sources

- 0%  Internet sources
- 5%  Publications
- 2%  Submitted works (Student Papers)

### Integrity Flags

#### 1 Integrity Flag for Review

-  **Replaced Characters**  
32 suspect characters on 8 pages  
Letters are swapped with similar characters from another alphabet.

Our system's algorithms look deeply at a document for any inconsistencies that would set it apart from a normal submission. If we notice something strange, we flag it for you to review.

A Flag is not necessarily an indicator of a problem. However, we'd recommend you focus your attention there for further review.

Susharma



# APPENDICES

## APPENDIX-1

### PROOF OF SCOPUS/SCI/SCIE INDEXING

The screenshot shows the Clarivate Master Journal List interface. The top navigation bar includes the Clarivate logo, a 'Products' menu, and a user welcome message 'Welcome, Aditi Sharma' with links for 'Settings' and 'Log Out'. The main navigation bar has tabs for 'Master Journal List', 'Search Journals', 'Match Manuscript', 'Downloads', and 'Help Center'. On the left, a sidebar menu lists 'General Information', 'Web of Science Coverage', 'Journal Citation Report', and 'Peer Review Information', with a 'Return to Search Results' button below. The main content area displays details for 'JOURNAL OF OPTICS-INDIA', including its ISSN (0972-8821 / 0974-6900), publisher (SPRINGER INDIA), and address. A 'General Information' table lists the journal website, publisher website, first year published (1972), frequency (Quarterly), issues per year (4), country/region (INDIA), and primary language (English). Below this, the 'Web of Science Coverage' section shows a table with columns for Collection, Index, Category, and Similar Journals, accompanied by a blue question mark icon.

The screenshot displays the Springer Nature Link page for the 'Journal of Optics'. The top navigation bar features the 'SPRINGER NATURE Link' logo, a 'Log in' button, and a search bar. Below the navigation bar, there are links for 'Find a journal', 'Publish with us', 'Track your research', and a search icon. The main content area has a dark blue header with the journal title 'Journal of Optics' and its publishing model 'Hybrid'. A 'Submit your manuscript' button is prominently displayed. To the right, the Springer logo is shown. At the bottom, there are links for 'Explore open access funding' and 'Select institution', and a footer with links for 'About this journal', 'Articles', and 'For authors'.

## APPENDIX-2

### COMMUNICATION RECORD

Fwd: : Submission Confirmation for Electromagnetic Wave Propagation through a Plasma Slab: Analysis of Reflection, Transmission, and Absorption Characteristics for varying mediums -



Suresh Sharma  
to me, Diya

19:23 (5 minutes ago) ☆ ☺ ↶ ⋮

**Prof. Suresh C. Sharma**  
Former Dean (Academic-PG)  
Former Head, Department of Applied Physics,  
Delhi Technological University (DTU),  
Govt. of NCT of Delhi,  
Shahbad Daultpur, Bawana Road, Delhi-110042, India  
Email: [suresh321sharma@gmail.com](mailto:suresh321sharma@gmail.com), [prof\\_sureshsharma@dtu.ac.in](mailto:prof_sureshsharma@dtu.ac.in)

Former Chairman, Department Research Committee(DRC)[Applied Physics] DTU, Delhi.  
Former Chairman, Board of Studies (BOS)[Applied Physics] DTU, Delhi  
Young Scientist Project Awardee (DST, Govt. of India).  
Monbusho Post-doctoral Fellowship Awardee (Govt. of Japan).  
JSPS (Invitation) Post-doctoral Fellowship Awardee (Govt. of Japan).  
Senior Research Associate under the Scientist's Pool Scheme Awardee (CSIR, Govt. of India).  
Commendable Research Award for Excellence in Research Awarded by DTU, Delhi for seven consecutive years i.e., March 21, 2018, March 19, 2019, March 13, 2020, February 15, 2021, March 3, 2022, April 6, 2023 & September 5, 2024.

----- Forwarded message -----

From: **Editorial Office** <[em@editorialmanager.com](mailto:em@editorialmanager.com)>

Date: Thu, 5 Jun 2025, 19:00

Subject: : Submission Confirmation for Electromagnetic Wave Propagation through a Plasma Slab: Analysis of Reflection, Transmission, and Absorption Characteristics for varying mediums - [EMID ]

To: Suresh Chandra Sharma <[suresh321sharma@gmail.com](mailto:suresh321sharma@gmail.com)>

Dear Plasma Physics Sharma,

Your submission entitled "Electromagnetic Wave Propagation through a Plasma Slab: Analysis of Reflection, Transmission, and Absorption Characteristics for varying mediums" has been received by Journal of Optics

You will be able to check on the progress of your paper by logging on to Editorial Manager as an author. The URL is <https://www.editorialmanager.com/opti/>.

The submission id is:

Please refer to this number in any future correspondence.

Thank you for submitting your work to our journal.

Kind regards,

Editorial Office  
Journal of Optics



Journal of Optics

Home

Submit a Manuscript

About

Help

#### Contributing Author Confirmation

Thank you for verifying your contributing authorship on "Electromagnetic Wave Propagation through a Plasma Slab: Analysis of Reflection, Transmission, and Absorption Characteristics for varying mediums" submitted by Suresh Chandra Sharma.

## APPENDIX-3

### LIST OF CONFERENCES

**Name of Conference:** The National Physics Conference (PHYCON-25)

**Conference Dates:** 2025, March 21-22

**Mode of the conference:** Offline

**Venue:** IIT ROPAR, RUPNAGAR, PUNJAB, INDIA

**Name of Conference:** International Conference on Advances in Nanomaterials and Nanotechnology (ICANN-2025)

**Conference Dates:** 2025, March 05-06

**Mode of the conference:** Offline

**Venue:** RAJDHANI COLLEGE, UNIVERSITY OF DELHI

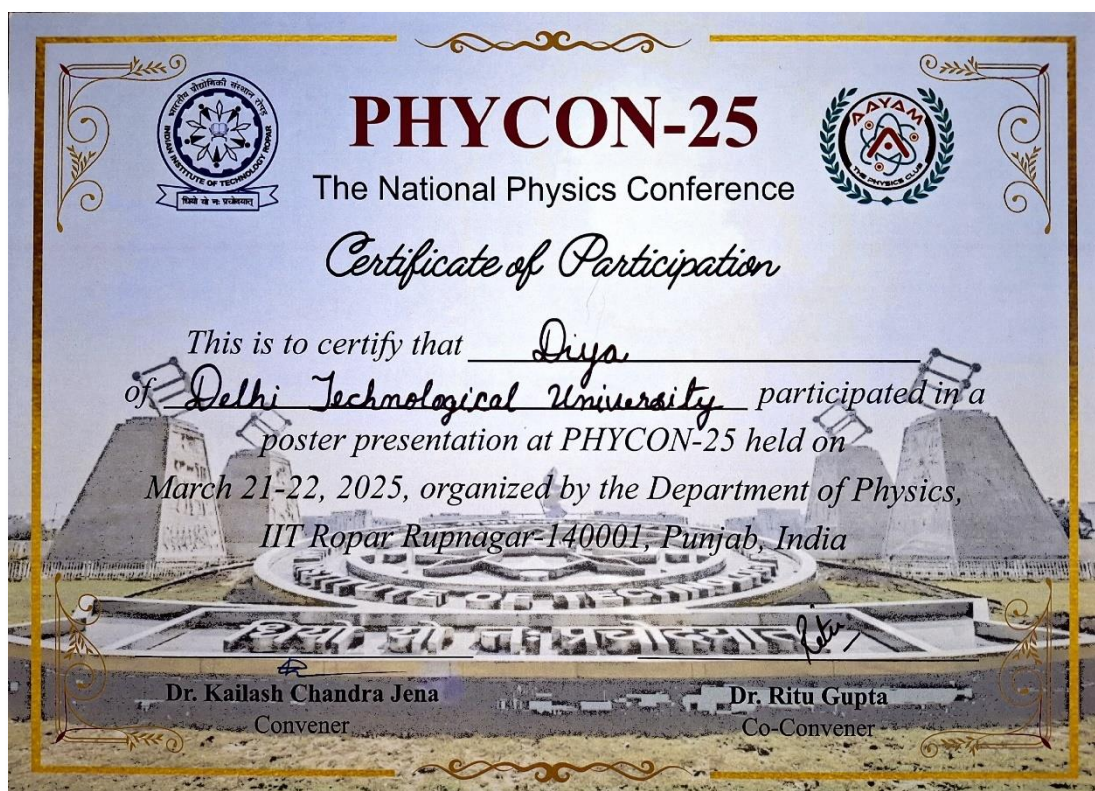
**Name of Workshop:** International Workshop on Cold Plasma Technology and Applications (CPTA-2025)

**Conference Dates:** 2025, February 06-08

**Mode of the conference:** Online

**Venue:** BIRLA INSTITUTE OF TECHNOLOGY MESRA, JAIPUR, RAJASTHAN, INDIA

## CONFERENCE PARTICIPATION CERTIFICATES









Sponsored by DRDO

## International Conference on advances in Nanomaterials and Nanotechnology (ICANN 2025)

BEST PAPER PRESENTATION AWARD

S.No. \_\_\_\_\_

This is to certify that Prof./Dr./Mr./Mrs. ADITI SHARMA

from DELHI TECHNOLOGICAL UNIVERSITY Chaired/Delivered Lecture/Participated/

Presented a paper titled ADVANCED THEORETICAL MODELING OF WAVE COEFFICIENTS & PHASE SHIFTS IN POLARISED LASER INTERACTION WITH STRATIFIED MEDIA

in the International Conference (ICANN 2025) held at Rajdhani College, University of Delhi on March 05-06, 2025.

  
**Prof. Rajesh Giri**  
 Principal, Rajdhani College

  
**Dr. Jasvir**  
 Convenor, ICANN-2025





Sponsored by DRDO

## International Conference on advances in Nanomaterials and Nanotechnology (ICANN 2025)

BEST PAPER PRESENTATION AWARD

S.No. \_\_\_\_\_

This is to certify that Prof./Dr./Mr./Mrs. DIYA


from DELHI TECHNOLOGICAL UNIVERSITY Chaired/Delivered Lecture/Participated/


Presented a paper titled ADVANCED THEORETICAL MODELING OF WAVE COEFFICIENTS & PHASE SHIFTS IN POLARISED LASER INTERACTION WITH STRATIFIED MEDIA

in the International Conference (ICANN 2025) held at Rajdhani College, University of Delhi on March 05-06, 2025.

  
**Prof. Rajesh Giri**  
 Principal, Rajdhani College

  
**Dr. Jasvir**  
 Convenor, ICANN-2025





Sponsored by DRDO

**International Conference on advances in Nanomaterials and Nanotechnology  
(ICANN 2025)**

**CERTIFICATE**


S.No PP58


This is to certify that Prof./Dr./Mr./Mrs. ADITI SHARMA

from DELHI TECHNOLOGICAL UNIVERSITY Chaired/Delivered Lecture/Participated/

Presented a paper titled ADVANCED THEORETICAL MODELLING OF WAVE CO-EFFICIENTS AND  
PHASE SHIFTS IN POLARISED LASER INTERACTION WITH STRATIFIED MEDIA

in the International Conference (ICANN 2025) held at Rajdhani College, University of Delhi on March 05-06, 2025.

  
**Prof. Rajesh Giri**  
 Principal, Rajdhani College

  
**Dr. Jasvir**  
 Convenor, ICANN-2025





Sponsored by DRDO

**International Conference on advances in Nanomaterials and Nanotechnology  
(ICANN 2025)**

**CERTIFICATE**

S.No PP61

This is to certify that Prof./Dr./Mr./Mrs. DIYA

from DELHI TECHNOLOGICAL UNIVERSITY Chaired/Delivered Lecture/Participated/

Presented a paper titled ADVANCED THEORETICAL MODELING OF WAVE COEFFICIENTS AND PHASE  
SHIFTS IN POLARISED LASER INTERACTION WITH STRATIFIED MEDIA

in the International Conference (ICANN 2025) held at Rajdhani College, University of Delhi on March 05-06, 2025.

  
**Prof. Rajesh Giri**  
 Principal, Rajdhani College

  
**Dr. Jasvir**  
 Convenor, ICANN-2025

